RING EFFECT STUDIES FOR A CLOUDY ATMOSPHERE USING GOME DATA

R. de Beek, M. Vountas, V. V. Rozanov, A. Richter, and J. P. Burrows

Institute of Environmental Physics, University of Bremen FB1, P.O. Box 330440, 28334 Bremen, Germany

Email:

Ruediger.de_Beek@iup.physik.uni-bremen.de
Marco.Vountas@iup.physik.uni-bremen.de
Vladimir.Rozanov@iup.physik.uni-bremen.de
Andreas.Richter@iup.physik.uni-bremen.de
John.Burrows@iup.physik.uni-bremen.de

1 Introduction

The fact that the depth of solar Fraunhofer lines in scattered light is less than those observed in direct sunlight, was discovered by Shefov [1959] [17] and Grainger and Ring [1962] [6] and is known as the "Ring Effect" or "Filling-in". Several publications analysed this effect and its origins, showing that rotational Raman scattering provides the dominant contribution to the Ring Effect [1, 10, 4, 5, 8, 3, 18]. The majority of these studies however concentrated on cloud-free conditions.

Detailed investigations of the effect of trace gas absorption and particle and cloud scattering requires a radiative transfer model, including rotational Raman scattering. Vountas et al. [1998] [18] introduced a new method to calculate Ring spectra by multiple scattering radiative transfer calculations, using the radiative transfer model SCIATRAN (formerly GOMETRAN) [16]. Vountas et al. [1998] demonstrated that by taking rotational Raman scattering into account within the radiative transfer processing, including trace gas absorption and aerosol and Rayleigh scattering, the filling-in of Fraunhofer and gas absorption features, resulting from rotational Raman scattering, explains to a high accuracy the Ring effect for cloud-free conditions. SCIATRAN is also able to model clouds as layers and as reflecting boundaries [12]. The modelling accounts for scattering mechanisms like Rayleigh-, Mie-, and Raman-scattering, and as a consequence influences on the slant path of the light (e.g. due to multiple scattering), strongly affecting filling-in of spectral structures. Excluding horizontal inhomogenities and polarisation, which can not yet be modelled with SCIATRAN, this enables the Ring Effect arising from clouds to be extensively investigated for both ground and satellite geometry.

In this study radiances between 390 nm and 400 nm were calculated including Ring in the cloudy atmosphere, and were compared to those from satellite borne observations where distinct Ring features appear. An investigation of the sensitivity of the retrieval of NO_2 from modelled spectra using the widely spreaded DOAS (Differential Optical Absorption Spectroscopy) technique [15] has been used to investigate different cloud scenarios with varying cloud types and heights.

The objective of the study is to support that our current understanding of physical processes, which determine the Ring Effect, is adequate to explain the observations from satellite spectrometers under cloudy conditions. Further such investigations are needed to gain a more general picture of the Ring Effect in the presence of clouds.

2 Ring Modelling and its Validation

Measurements of the Global Ozone Monitoring Experiment GOME [2] were selected for comparison with spectra simulated with SCIATRAN. The spectral range between 390 nm and 400 nm was selected as the test region, because the weak absorption features do not interfere significantly with two strong solar Fraunhofer lines, which are the CaII-lines, located at 393.37 nm and 396.85 nm.

A solar irradiance spectrum I_0 is required for the modelling of the Ring filling-in structures. The high resolution solar spectrum measured by Kurucz et al. [1984] [13], convolved with the instrument function, was used. For both modelled and measured spectra, we define the Differential Optical Depth, DOD, as

$$DOD = \ln I/I_{ref} - P \,, \tag{1}$$

where I is the radiance and $I_{ref} = I_0$. A polynomial of third order, P, accounting for the broadband features in the considered spectral region, is subtracted. In the selected spectral region, DOD can be expected to contain predominantly Ring. Wavelength dependent least-squares fitting was performed to account for wavelength calibration discrepancies.

2.1 Comparison with Satellite Measurements

For the 15th of October 1996, a specific GOME pixel was chosen for comparison, where a large cloud field passed the observed area. The GOME spectrum was measured at 43.23 N, 27.44 W, at 12.52 h UTC. This measurements were chosen as timely and spatially near-coincident temperature measurements from Meteosat and a Polarstern sonde were made available, enabling independent estimates of a mean cloud-top temperature and height. The GOME ground pixel was identified to be totally cloud covered using the GOME operational cloud coverage product. The cloud coverage value for this GOME ground pixel is 1.0 (100%).

An average cloud-top height according to the GOME observation was derived from cloud-top temperatures using the Meteosat data, detected at 12.00 h UTC and temperature measurements of the balloon sonde, which was launched from the German research ship Polarstern at 42 N, 35 W, at 10.18 h UTC. The Meteosat data was spatially filtered using the area observed by GOME and taken the movement of the cloud field between the different measurement times into account, estimated using the Polarstern sonde wind speed data. Comparison of both the sonde temperature profile and the derived Meteosat cloud-top temperature yields a mean cloud-top height of about 7 km $\pm$1 km.

Adequate radiances were calculated with SCIATRAN. For comparison with the modelled radiance, the GOME pixel was assumed to be homogeneously cloud covered. From Figure 1 it can be seen, that for a model cloud with a cloud-top height of 7 km and a cloud optical thickness 5 the resulting Ring structure around 393.5 nm is in good agreement with the experiment.

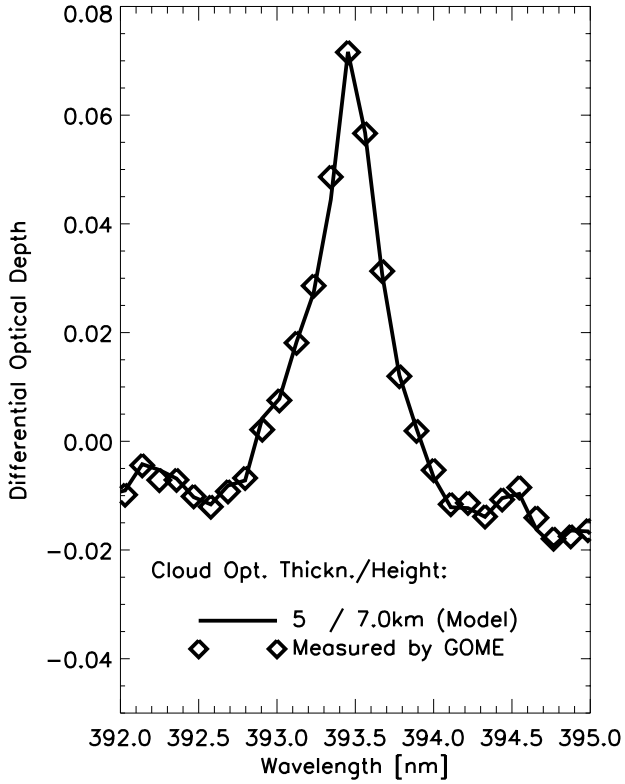

Figure 1: DODs derived for the spectral range from 390 nm to 400 nm from a GOME observation on the 15th of October 1996 at 43.23 N, 27.44 W, 12.52 h UTC, solar zenith angle 52.9deg, identified to be homogeneously cloud covered. Dotted line is a model calculation using a standard nimbostratus cloud reaching from 5 to 7 km height with optical thickness 5.

2.2 Influence of Cloud-top Height and Cloud Optical Thickness

Combinations of cloud-top height and cloud optical thickness can yield filling-in similar to those in the upper section. This is demonstrated using calculations of filling-in measures defined by

$$R = OD_l + (\lambda_c - \lambda_l) * \frac{(OD_r - OD_l)}{(\lambda_r - \lambda_l)} - OD_c$$

using optical depths (OD) at the line center λ_c and at two spectral points of the continuum ($\lambda_l = 392.39\,nm$ and $\lambda_r = 394.21\,nm$, see e.g. Joiner and Bhartia [1995] [9]). These quantities are furtheron called "Ring Amplitudes" and are measures of the strength of the filling-in.

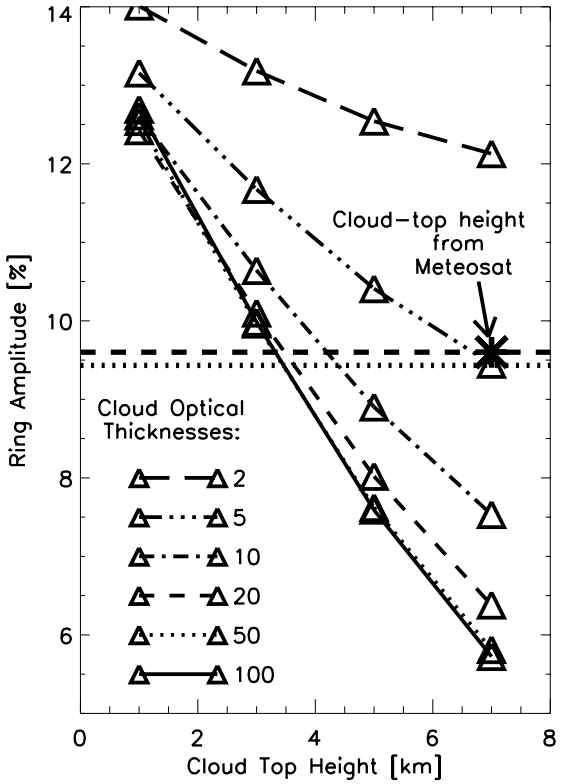

Figure 2: Ring amplitude versus Cloud-Top-Height for Clouds with different optical thicknesses as calculated with SCIATRAN for the CaII Fraunhofer line Ring structure at 393.37 nm. The $*$ indicates the cloud-top height as estimated using near-coincident Meteosat (DWD, Germany) and balloon sonde temperatures (AWI, Germany). This fits an optical thickness of the cloud of about 5. The dashed and dotted horizontal lines indicate measured and best modelled Ring Amplitudes, respectively (see text).

Ring Amplitudes calculated for different cloud optical thicknesses and cloud-top heights are shown in Figure 2. The Ring amplitude derived from the measured GOME DOD is about 9.6 % of the radiance. This corresponds to a cloud-top height of 7 km when assuming a cloud optical thickness of about 5 as has been shon above (Figure 1). Other solutions having the same Ring Amplitude are indicated in Figure 2 by a horizontal dashed line. It can be seen that several combinations of the physical atmospheric parameters in the model can fit the measurements, thus providing realistic results.

More conclusions can be gained from Figure 2. The model Ring spectrum for a given wavelength is defined by [18]

$$R \;=\; \ln I^+ / I^- \;, \tag{2}$$

where for the calculation of the atmospheric radiance I^+, rotational Raman scattering is included, whereas for I^- it is not. R can be approximated by

$$R \;\approx\; \Delta I / I^- \;, \tag{3}$$

where $\Delta I = I^+ - I^-$ is the Raman-scattering contribution. From Figure 2 it can be seen that the Ring Amplitude increases with decreasing cloud optical thickness. The slant path of the light is enhanced within the cloud the deeper the radiation can penetrate into it (supported by slant path enhancement due to multiple scattering) and below the cloud. The decrease of optical thickness goes with an increase of Rayleigh scattering events, having Raman-scattering contributions, inside and below the cloud, leading to increasing Ring Amplitudes. For thin clouds, ΔI in Equation (2) increases in the center of the considered Fraunhofer line, i.e. filling-in is enhanced. In the clear sky case the filling-in is strongest (in case of satellite geometry).

A cloud with optical thickness of more than ≈50 almost completely cuts off the atmosphere below the cloud-top height when looking from a satellite. Higher optical thicknesses do not lead to further decrease of the filling-in (Figure 2). This effect is amplified through the fact, that the filling-in increases with decreasing cloud reflectivity due to Mie-scattering. In Equation (2) R is enhanced by a decrease of Mie-scattered radiance. For the same reason the observed increase of radiance by Mie-scattering in case of optical thick clouds weakens the Ring amplitude compared to the clear sky.

An increase of the cloud-top height leads to decreasing filling-in, as the cloud cuts off more atmospheric volumn, devreasing the number of Rayleigh-scattering events. With the above it is obvious, that this feature is less distinct for optical thinner clouds.

In satellite geometry most of the observed light is reflected from the top layers of the cloud in case of a large cloud optical thickness. Changes of the Ring effect due to clouds therefore depend more on the cloud-top height. Retrievals of cloud-top heights are then possible using the known relation to the Ring amplitudes as shown e.g. in Fig. 2. With the restriction to optically thick clouds this has already been demonstrated by Joiner and Bhartia [1995] [9]. However, for a smaller cloud optical thickness more light penetrates into and through the cloud leading to significant changes of the Ring amplitudes, which suggests lower cloud-top heights if no additional information on the cloud optical thickness is applied.

3 Using Ring and O2 Structures Simultaneously with Optical Depth

Additional information on cloud-top height is provided by O_2 differential absorption structures as measured by GOME [14, 7, 11]. The absolute optical depth contain in addition information about the cloud optical thickness. First approaches using O_2 information arround 761 nm simultaneously with Ring modelling have shown, that in this case, a two cloud layer modelling yields a solution consistent with all mentioned parameters as measured by GOME in the considered case study. An altostratus between 6.5 and 7 km (cloud optical thickness=6) and a nimbostratus cloud between 2 and 3 km (cloud optical thickness=20) was found to yield the best solution of the considered parameter sets. Figure 2 shows the according differential optical depth and optical depth calculated using the considered GOME measurement (see Fig. 1) and from model radiances, calculated with SCIATRAN. The thin model cloud (optical thickness 6) with cloud-top height at 7 km fits well the differential structure of the O_2 bands, whereas the optical density is too high (cloud too dark). The thicker model cloud (optical thickness 20) with cloud-top height at 3 km almost fits the optical density but with a too deep differential structure. In this case the O_2 absorption is comparable to those of the clear sky case. Surely the cloud shields part of the atmospheric Rayleigh scattering volumn, leading to a decrease of filling-in. On the other hand the increase of filling-in due to an enhancement of the slant path inside of the moderately optical thick cloud compansates this effect.

The two layer approach is the best choise of all considered cases given best fits for optical and differential optical depth and the considered Ca II Ring structure, simultaneously. The Ring amplitude is shown in Figure 2 (dotted line). It has to be further investigated if information about vertical inhomogeneity could be retrieved using GOME data containing Ring and O_2 A band structures and according absolute optical depth measurements.

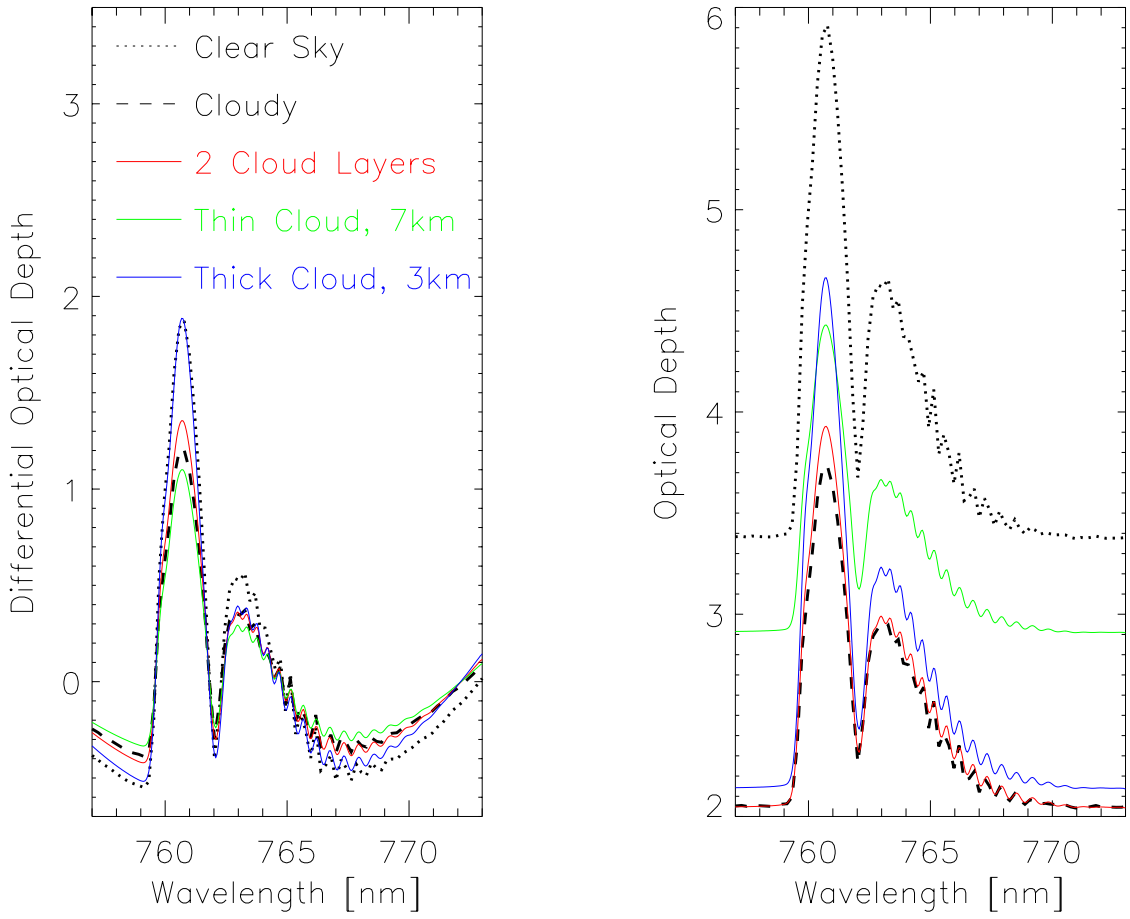

Figure 3: Differential optical depth and optical depth calculated from GOME measurements (see Fig. 1) and from model radiances, calculated with SCIATRAN. The thin model cloud (green curve, optical thickness 6) with cloud-top height at 7 km fits well the differential structure of the O_2 bands, whereas the optical density is too high (cloud too dark). The thicker model cloud (blue curve, optical thickness 20) with cloud-top height at 3 km almost fits the optical density but with a too deep differential structure (as deep as for the clear sky!). The two layer approach is the best choise of all considered cases given best fits for optical and differential optical depth and the Ca II Ring structure, simultaneously.

4 NO_2 Retrieval Sensitivity to Clouds

When using different cloud scenarios the modelled Ring spectra show wavelength dependent differences, mainly arising from different trace gas slant columns along the slant of the light path and therefore different filling-in of molecular absorption structures. Inadequate Ring spectra used when fitting radiances to retrieve NO_2 vertical columns can therefore lead to errors in the trace gas retrieval. These errors depend on the slant path within the cloud in conjunction with the number of Rayleigh scattering events, enhancing the trace gas absorption and the Ring amplitude, respectively.

Model radiances, calculated using variable cloud parameters, have been used as input for a DOAS fit, using the same absorption cross-sections and the same solar spectrum than for the modelling but different Ring spectra. The vertical column retrieval results using a spectral range between 425nm and 450nm have been compared with those derived from the trace gas scenario profile used for the modelling.

In this part both ground-based and satellite geometry have been investigated. For the ground-based case it has been shown that the errors depend mainly on the cloud optical thickness and the cloud heigth extension. For example cloud radiances retrieved with clear sky Ring (60° solar zentih angle) show errors of about -4 % and up to -9 % for very thick clouds. This case considered in satellite geometry gives errors of -3 % which mainly arises due to the difference in SZA. Using a clear sky Ring spectra adequate wrt. SZA leads up to 1 % error using a high cloud.

5 Conclusions

For the cases studied where reasonable knowledge of the local conditions exists, it was shown that SCIATRAN reproduces well the Ring spectra considering clouds and Ring effects for satellite observations. This has been demonstrated by comparisons of the model to measurements taken with the satellite instrument GOME.

For the NO_2 retrieval it can by stated that Ring spectra which are inadequate wrt. clouds have minor consequences in the satellite case whereas for the ground-based situation thick clouds (nimbostratus and cumulonimbus) can have significant impact on the retrieval results given errors around 4-6 % in vertical column. The effect increases for smaller solar zenith angles.

This study led to a better understanding of the variations of the Ring effect under the influence of clouds in satellite geometry. Clouds can lead to both increasing and decreasing Ring amplitudes, depending on cloud optical thickness and cloud top height. These parameters can be potentially retrieved from GOME UV/visible spectra using Ring and O_2 absorption structures, and absolute reflectivities, simultaneously, in conjunction with radiative transfer models such as SCIATRAN.

Acknowledgements We thank the Deutscher Wetterdienst, Germany, for making METEOSAT pictures available and the Alfred Wegener Institute for Polar and Marine Research for providing sonde temperature data. Part of this work was funded by the University of Bremen, and the State Bremen.

References

[1] Brinkmann, R. (1968). Rotational Raman scattering in planetary atmospheres. *The Astrophysical Journal*, 154:1087–1093.

[2] Burrows, J., Weber, M., Buchwitz, M., Rozanov, V. V., Ladstädter-Weissenmayer, A., Richter, A., de Beek, R., Hoogen, R., Bramstedt, K., Eichmann, K.-U., Eisinger, M., and Perner, D. (1999). The Global Ozone Monitoring Experiment (GOME): Mission concept and first scientific results. *Journal of the Atmospheric Sciences*, 56:151–171.

[3] Burrows, J. P., Rozanov, V. V., Vountas, M., Richter, A., Platt, U., Haug, H., Marquard, L., and Chance, K. (1996). Study of the ring effect (final report). European Space Agency/ESTEC, ESA Contract 10996/94/NL/CN.

[4] Clarke, D. and Basurah, H. (1989). Polarisation measurements of the Ring effect in the daytime sky. *Planetary and Space Science*, 37:627–630.

[5] Fish, D. and Jones, R. (1995). Rotational Raman scattering and the Ring effect in zenith-sky spectra. *Geophysical Research Letters*, 22(7):712–716.

[6] Grainger, J. F. and Ring, J. (1962). Anomaleous Fraunhofer line profiles. *Nature*, 193:762.

[7] Guzzi, R., Burrows, J., Cattani, E., Cervino, M., Kurosu, T., Levoni, C., and Torricella, F. (1998). Gome cloud and aerosol data products algorithms development. Technical Report ESA Contract 11572/95/NL/CN, European Space Agency, ESA/ESTEC, PO Box 299, 2200 AG Noordwijk, The Netherlands.

[8] Joiner, J., Barthia, P., Cebula, R., Hilsenrath, E., McPeters, R., and Park, H. (1995). Rotational Raman scattering (Ring effect) in satellite backscatter ultraviolet measurements. *Applied Optics*, 34(21):4513–4525.

[9] Joiner, J. and Bhartia, P. (1995). The determination of cloud pressures from rotational Raman scattering in satellite backscatter ultraviolet measurements. *J. Geophys. Res.*, D11(100):23019–23026.

[10] Kattawar, G., Young, A., and Humphreys, T. (1981). Inelastic scattering in planetary atmospheres, I, the Ring effect, without aerosols. *The Astrophysical Journal*, 243(3):1049–1057.

[11] Kurosu, T., Chance, K., and Spurr, R. J. D. (1999). CRAG – cloud retrieval algorithm for the European Space Agency's Global Ozone Monitoring Experiment. In *ESAMS '99 - European Symposium on atmospheric Measurements from Space*, volume 2, pages 513–521, Noordwijk, The Netherlands. ESA Earth Sciences Devision, ETEC. 18.–22. January 1999.

[12] Kurosu, T., Rozanov, V. V., and Burrows, J. P. (1997). Parameterization schemes for terrestrial water clouds in the radiative transfer model GOMETRAN. *Journal of Geophysical Research*, 102(D18):21809–21823.

[13] Kurucz, L. R., Furenlid, I., Brault, J., and Testerman, L. (1984). Solar flux atlas from 296 to 1300 nm. Technical report, National Solar Observatory, Sunspot, New Mexico. Technical Report.

[14] Kuze, A. and Chance, K. V. (1994). Analysis of cloud top height and cloud coverage from satellites using the o $_2$ a and b bands. *Journal of Geophysical Research*, 99(D7):14481–14491.

[15] Platt, U. and Perner, D. (1980). Direct measurement of atmospheric HCHO, HNO_2, O_3, NO_2 and SO_2 by differential optical absorption spectroscopy. *Journal of Geophysical Research*, 85.

[16] Rozanov, V. V., Diebel, D., Spurr, R. J. D., and Burrows, J. P. (1997). GOMETRAN: A radiative transfer model for the satellite project GOME, the plane-parallel version. *Journal of Geophysical Research*, 102(D14):16683–16695.

[17] Shefov, N. (1959). Spectroscopic, photoelectric, and radar investigations of aurorae and the nightglow. *Izd. Akad. Nauk*, 1(25). in Russian.

[18] Vountas, M., Rozanov, V., and Burrows, J. (1998). Ring effect: Impact of rotational raman scattering on radiative transfer in earth's atmosphere. *Journal of Quantitative Spectroscopy and Radiative Transfer*, 60(6):943–961.